



# WPI

## **Phosphatidylinositol Phase Behavior in the Presence of Bivalent Cations**

A Major Qualifying Project Report Submitted to the Faculty of  
WORCESTER POLYTECHNIC INSTITUTE  
In partial fulfillment of the requirements for the  
Degree of Bachelor of Science in Biochemistry

Written by:

Approved by:

---

Safiya Ali

---

Dr. Arne Gericke

April 2023

*This report represents the work of one or more WPI undergraduate students submitted to the faculty as evidence of completion of a degree requirement. WPI routinely publishes these reports on the web without editorial or peer review*

## Table of Contents

List of Figures .....	3
List of Tables .....	4
Acknowledgments.....	5
Abstract.....	6
1.0 Introduction & Background.....	7
1.1 Importance of Biological Membranes.....	7
1.2 Fluid Mosaic Model .....	7
1.3 Structure of Phospholipids .....	8
1.4 Lipids Content of Plasma Membrane.....	8
1.5 Importance of Phosphoinositides .....	9
1.6 Studying Lipids via Model Membranes.....	9
1.7 Membrane Phase Behavior.....	10
1.8 Differential Scanning Calorimetry.....	11
1.9 Objectives of this Study .....	12
2.0 Materials and Methodology .....	13
2.1 Materials.....	13
2.2 Sample Preparation .....	13
2.3 Differential Scanning Calorimetry .....	13
3.0 Results.....	15
3.1 DPPI Results .....	15
3.2 Liver PI Results.....	17
3.3 Comparison of Anionic Lipids and Bivalent Cations .....	18
4.0 Discussion.....	20
4.1 Comparison of the Phase Transition Temperature of DPPI vs Liver PI .....	20
4.2 Comparison of the Phase Transition Temperature of Calcium vs Magnesium.....	20
5.0 Conclusion & Future Studies .....	22
6.0 References.....	23

## List of Figures

**Figure 1.** Fluid Mosaic Model *7*

**Figure 2.** Structure of 1,2-dipalmitoyl-sn-glycero-3-phospho-(1'-myo-inositol) *8*

**Figure 3.** Structure of L- $\alpha$ -phosphatidylinositol (Liver, Bovine) *8*

**Figure 4.** Classification of model membrane based on their size and number of lipid layers *10*

**Figure 5.** Schematic of Differential Scanning Calorimetry *11*

**Figure 6.** Differential Scanning Calorimeter as seen in the Gericke Lab *14*

**Figure 7.** DSC thermograms of DPPI MLVs *15*

**Figure 8.** DSC thermograms of DPPI-Ca<sup>2+</sup> MLVs *16*

**Figure 9.** . DSC thermograms of DPPI-Mg<sup>2+</sup> MLVs *16*

**Figure 10.** DSC thermograms of Liver PI-Ca<sup>2+</sup> MLVs *17*

**Figure 11.** DSC thermograms of Liver PI-Mg<sup>2+</sup> MLVs *17*

**Figure 12.** DSC thermograms of DPPI Standard, DPPI-Ca<sup>2+</sup>, and DPPI-Mg<sup>2+</sup> MLVs *18*

**Figure 13.** DSC thermograms of Liver PI-Ca<sup>2+</sup> and Liver PI-Mg<sup>2+</sup> MLVs *19*

**Figure 14.** Fatty acid distribution of Liver PI *20*

## List of Tables

**Table 1.** Summation of the gel/fluid phase transition temperature of DPPI and Liver PI in the presence (and absence of DPPI) of  $\text{Ca}^{2+}$  and  $\text{Mg}^{2+}$  **19**

## Acknowledgments

I would like to express my deepest gratitude and appreciation to all those who have helped and supported me throughout this project.

My sincere gratitude to Dr. Arne Gericke, for giving me the opportunity to work in his lab for the entirety of my undergraduate studies. His unwavering guidance and support have greatly shaped me into the scientist I am today.

I would like to thank the members of the Gericke lab who have generously given me their time and provided valuable insight into this study. In particular, Trevor Paratore for always being willing to help in any capacity from double checking my calculations to data analysis and Peter Oni for his continuous support.

I would also like to extend my heartfelt gratitude to my family and friends for their endless support and encouragement throughout this journey. Their love, patience and understanding have been a constant source of inspiration and motivation to me.

This work was supported by the National Science Foundation (CHE 1904886).

## Abstract

Phosphatidylinositol (PI) has pivotal roles in many cellular signaling events. Due to their anionic nature, these lipids interact with bivalent cations and the cationic parts of proteins. We are investigating the phase behavior of anionic lipids in the presence of  $\text{Ca}^{2+}$  or  $\text{Mg}^{2+}$  cations using differential scanning calorimetry (DSC) of multilamellar vesicles. For diplamitoylphosphatidylinositol (DPPI) vesicles, we found in pH 7.2 buffer a phase transition temperature of  $43.6^\circ\text{C}$ , while in the presence of  $\text{Ca}^{2+}$  and  $\text{Mg}^{2+}$  the phase transition temperature shifted to  $55.8^\circ\text{C}$  and  $51.6^\circ\text{C}$ , respectively. For Liver phosphatidylinositol (Liver PI), we found in pH 7.2 buffer in the presence of  $\text{Ca}^{2+}$  and  $\text{Mg}^{2+}$  the phase transition temperature to be  $11.8^\circ\text{C}$  and below  $0^\circ\text{C}$ , respectively.

## 1.0 Introduction & Background

### 1.1 Importance of Biological Membranes

Biological membranes, which are made up of both lipids and proteins, play a critical part in all cellular processes, including cell signaling and nutrient flow. While proteins are in charge of carrying out diverse membrane tasks, lipids supply the basic structure of the membrane as well as the ideal conditions for the proteins to carry out their duty. Biological membranes exist in an aqueous environment that is rich in small ionic species.

### 1.2 Fluid Mosaic Model

Proposed in 1972, Singer and Nicolson's Fluid Mosaic Membrane Model of biological membrane structure was a fundamental framework model for understanding membrane proteins and lipids, as well as their dynamics [1]. The model accounted for other properties such as membrane asymmetry and lateral mobility of membrane components [3]. The proteins that are integral to the membrane are a heterogenous set of globular molecules, arranged in an amphipathic structure, with the ionic and highly polar group protruding from the membrane into the aqueous phase and the non-polar groups largely buried in the hydrophobic interior. Said molecules are partially immersed in a phospholipid matrix which is arranged as a discontinuous, fluid bilayer, although only a small percentage of the lipids may interact specially with the membrane proteins [2]. The formation itself is driven by the thermodynamics of hydrophobic and hydrophilic interactions to minimize the free energy of the structure. To this day, it serves as the basis of our interpretation of membrane structure, although it has evolved and has been refined as additional studies report further complexities such as lipid rafts and protein complexes in addition to membrane-associated cytoskeletal structure and extracellular matrix which limits protein mobility and range [1]. Simply put, the membrane is a highly complex and heterogenous environment [6].

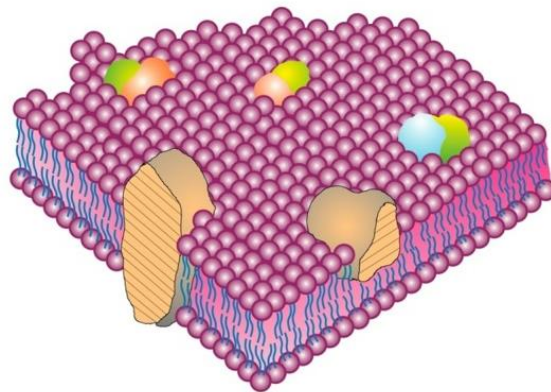


**Figure 1.** Fluid Mosaic Model from Nicolson & Ferreira’s 2021 review paper titled “A Brief Introduction to Some Aspects of the Fluid-Mosaic Model of Cell Membranes Structure and Its Importance in Membrane Lipid Replacement.”

### 1.3 Structure of Phospholipids

The structure of phospholipids is integral to the basic functioning of membranes. Two fatty acid tails and a phosphate group head make up a phospholipid. Fatty acids are long chains of hydrogen and carbon whereas phosphate groups are made up of a phosphorus molecule with oxygen molecules attached [15]. The tails often vary in length but are typically 14-24 carbon atoms [15]. These two phospholipid components are linked by a third molecule, glycerol.

The phosphate group head is hydrophilic and the fatty acid tails are hydrophobic meaning that head groups form favorable electrostatic interaction or hydrogen bonds with water molecules whereas the fatty acid tails cannot form energetically beneficial interaction with water [15]. As for reasons just stated lipid molecules spontaneously bury their hydrophobic tails in the interaction and expose their hydrophilic heads to water. Depending on shape, this can be accomplished in two ways: (1) they may create spherical micelles with the tails inward or (2) they can form lipid bilayers with the hydrophobic tails sandwiched between the hydrophilic head groups [15].

Different headgroups are characterized by different charges (negative vs. zwitterionic) show varying abilities to engage in hydrogen bonding [15]. Differences in length and saturation of fatty acid tails are significant because they alter the capacity of phospholipid molecules to pack, influencing membrane fluidity [15].

Lipid bilayers are selectively permeable meaning that only particular components may pass through them to enter or exit. This keeps the content of the cell or aqueous area function correctly and separates the inside of the cell from the outside environment.

### 1.4 Lipids Content of Plasma Membrane

The lipid and protein makeup of the plasma membrane differs between cell types. Additionally, the plasma membrane is divided into microdomains with distinct physicochemical features. Both leaflets of the plasma membrane in eukaryotes have distinct lipid composition [18].

Plasma membranes are primarily made of four phospholipids: phosphatidylcholine, phosphatidylethanolamine, phosphatidylserine, and sphingomyelin [11]. Phosphatidylinositols are a small component of the plasma membrane but they are vital for cell signaling processes. They are distributed asymmetrically throughout the membrane bilayer [11].

The three main functions cells depend upon lipids is for energy storage, compartmentalization, and signaling

### 1.5 Importance of Phosphoinositides

Phosphoinositides (PIPs) account only for a small percentage of the cellular membrane in eukaryotic cells, however, they control a tremendous array of cellular signaling events [8]. Discovered and studied in the 1970s and 1980s as plasma membrane signaling molecules, research followed that explored the wider range of biological processes regulated by PIPs [9]. PIPs are responsible for regulating vesicular trafficking, modulating lipid distribution and metabolism, regulating ion channels, pumps, and transporters, and controlling both endocytosis and exocytosis processes [9]. Other locations that PIPs reside include endoplasmic reticulum, early and late endosomes, trans-Golgi, and secretory granules [8].

This project will focus on 1,2-dipalmitoyl-sn-glycero-3-phospho-(1'-myo-inositol) (DPPI) and L- $\alpha$ -phosphatidylinositol (Liver, Bovine) (Liver PI) which are depicted below.

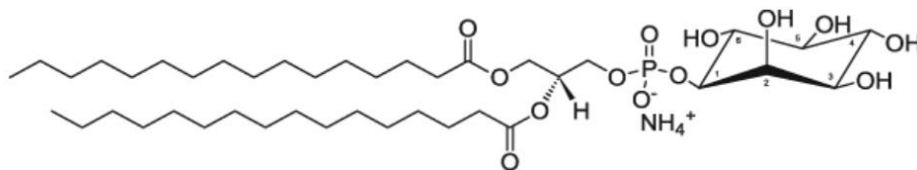


**Figure 2.** Structure of 1,2-dipalmitoyl-sn-glycero-3-phospho-(1'-myo-inositol) also known as DPPI (16:0 PI) from Avanti Polar Lipids [13].

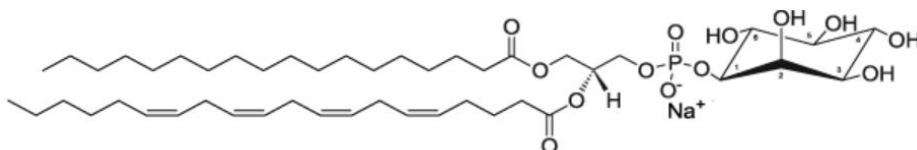


**Figure 3.** Structure of L- $\alpha$ -phosphatidylinositol (Liver, Bovine) also known as Liver PI from Avanti Polar Lipids [14].

### 1.6 Studying Lipids via Model Membranes

Lipids are the building block of biological membranes and by studying lipid phase behavior, researchers have discovered its relevance to major structural functions and their varied roles. The major discovery that the biomembrane is a liquid-crystalline lipid bilayer with proteins embedded has been a hallmark in membrane biophysics [7].

Biological membranes have a high degree of complexity which makes studying specific interactions and engagements a challenge. Therefore, due to its simplicity and ability to tune the environment, model membranes are ideal to characterize the phase behavior of a variety of lipids [4]. It should be noted that observations from model membranes might or might not translate into a biological system as there are a plethora of additional cellular components. Studies conducted

in models should be treated as a snapshot of lipids' favored behavior which in turn enhances our knowledge of how lipids may interact in the plasma membrane [4]. Types of model membranes include micelles, multilamellar vesicles, small unilamellar vesicles, large unilamellar vesicles, giant unilamellar vesicles, and supported lipids [4].

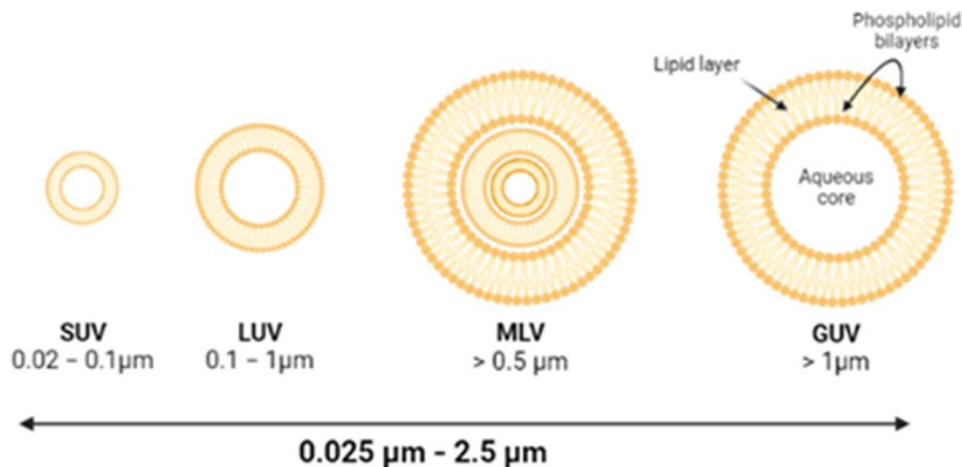


**Figure 4.** Classification of model membranes based on their size and number of lipid layers from N ria Garr s et al. 2022 article titled, “Baricitinib Liposomes as a New Approach for the Treatment of Sj gren’s Syndrome” [12].

### 1.7 Membrane Phase Behavior

Lipids self-assemble in a number of phases as a function of their structure in combination with other variables such as water content, temperature, pressure, and aqueous phase compositions. Lipid phases are characterized by their symmetry, hydrocarbon chain arrangement, and curved mesomorphic phase [7]. For membrane lipids, the general seven temperature dependent phase transitions are lamellar crystalline subgel, to lamellar gel, lamellar liquid-crystalline, bilayer cubic, inverted hexagonal, inverted micellar cubic, and inverted micellar [7].

From the biological standpoint, transitions involving the physiologically important lamellar liquid-crystalline phase is of most interest. This is the major energetic event in the lipid bilayer with the largest enthalpy change as it’s the energy required to expand the hydrocarbon chain and increase bilayer area [7]. The temperature/melting transition can be measured using Differential Scanning Calorimetry, Pressure Perturbation Calorimetry (PPC), or Isothermal Titration Calorimetry (ITC).

Studying the phase behavior of biological members is best done by studying simple bilayer mixtures with as few as three components and is key to understanding membrane-bound protein’s activity, access, and targets. Characteristics of the phase depends on several variables such as temperature, pressure, composition, pH, ionic strength, and presence of particular

multivalent ions [5]. Symmetric bilayers are typically studied over asymmetric bilayers as preparing asymmetric layers in vitro is challenging and because mixtures that model the outer leaflet give rise to different coexisting lipid phases [6]. Researchers are mainly interested in how membrane composition and tweaking different variables will influence how proteins cluster which in turn can influence enzymatic activities.

The two main factors that largely determine the phase transition temperature is the length of the hydrocarbon chains – the longer and more saturated the chain is, the higher the transition temperature. Regarding lipids with unsaturated chains, the positions and numbers of the double bond determined the phase transition temperature. Additionally, the linkage between the chains and the polar head group plays a role [7].

Lipid phase behavior is also determined by composition of lipid mixtures. Another variable that affects the lipid phase behavior is change of pH which can protonate or deprotonate the lipid head group which affects the surface charge of the membrane [7]. Protonation decreases lipid hydration and therefore will increase the phase transition temperature. [7]

### 1.8 Differential Scanning Calorimetry

Calorimetry is a primary technique for measuring the thermal characteristics of materials in order to create a link between temperature and certain physical properties of substances. Differential scanning calorimetry (DSC) is the most popular form of calorimeter. It is a thermal analysis instrument that measures how the physical characteristics of a sample change as temperature is changed. It is determined using the difference of the heat supplied between the sample and the reference during a controlled temperature increase or decrease. The melting of a phase requires more heat to increase the temperature of the sample cell relative to the reference cell, which results in an endothermic peak in the thermogram. DSC is therefore particularly useful for monitoring changes in phase transitions.

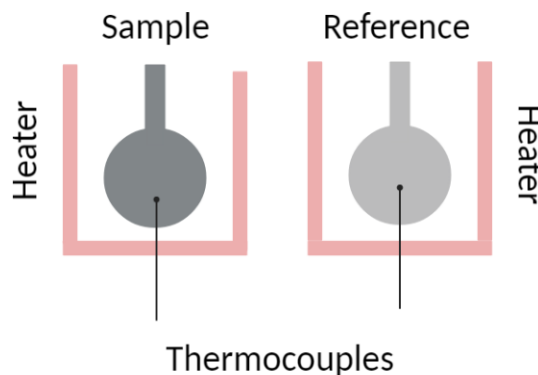


**Figure 5.** Schematic of Differential Scanning Calorimetry features a sample and reference channel. Sample channel includes sample and buffer whereas reference channel only includes

buffer. Channels are surrounded by heaters and are monitored by thermocouples. Computer schematic is not depicted. Original figure.

DSC is frequently used to study single molecular transitions of one conformation to another. Temperature of both cells are raised identically over time. The difference in the input energy required to match the temperature of the sample to that of the reference would be the amount of excess heat absorbed or released by the molecule in the samples. [10]

### 1.9 Objectives of this Study

For this project, we are investigating the phase behavior of anionic lipids, DPPI and Liver PI, in the presence (in the case of DPPI, absence) of  $\text{Ca}^{2+}$  or  $\text{Mg}^{2+}$  of multilamellar vesicles. We will visualize the behavior of DPPI and Liver PI using differential scanning calorimetry. We hypothesize that DPPI will have a greater phase transition temperature as compared to Liver PI and that  $\text{Ca}^{2+}$  will shift the phase transition temperature higher than  $\text{Mg}^{2+}$ .

## 2.0 Materials and Methodology

### 2.1 Materials

Dipalmitoylphosphatidylinositol (DPPI) and L- $\alpha$ -phosphatidylinositol (Liver, Bovine) (sodium salt) (Liver PI) were obtained from Avanti Polar Lipids (Alabaster, AL) with a formula weight of 828.1 g/mol and 902.1 g/mol, respectively (the purity of synthetic lipids as 99%). ACS grade chloroform and methanol were used to prepare lipid stock solutions (Fisher Scientific, Chicago, IL). Buffer 2-[4-(2-hydroxyethyl)piperazin-1-yl]ethane-1-sulfonic acid (HEPES) as well as ethylenediaminetetraacetic acid (EDTA), sodium chloride (NaCl), calcium chloride (CaCl<sub>2</sub>) and magnesium chloride (MgCl<sub>2</sub>), were of enzyme grade purity (Fisher Scientific, Chicago IL). Buffers had the general composition 150 mM NaCl, 10 mM HEPES 0.1 mM EDTA, 1 mM CaCl<sub>2</sub>/1 mM MgCl<sub>2</sub> and were adjusted to the physiological pH of 7.2 using aqueous HCl or KOH, respectively. The water used for buffer preparation was HPLC grade (Fisher Scientific, Chicago, IL).

### 2.2 Sample Preparation

DPPI and Liver PI lipids were stored in 2:1 chloroform/methanol stock solutions at concentrations of 0.630 mM and 2.77 mM, respectively. Multilamellar vesicles (MLVs) were prepared by transferring 190  $\mu$ L of DPPI or 289  $\mu$ L of Liver PI stock solutions into a 2 mL vial and quickly drying in a stream of dry nitrogen at an elevated temperature of  $\sim$ 65°C. The samples were dried in a high vacuum chamber at 45°C for at least 1 hour. DPPI lipid mixtures were resuspended in 800  $\mu$ L of warmed buffer solution (150 mM NaCl, 10 mM HEPES, 0.1 mM EDTA at pH 7.2 for standard experiment; 150 mM NaCl, 10 mM HEPES, 1 mM CaCl<sub>2</sub> at pH 7.2 for calcium experiment; pH 7.2, 150 mM NaCl, 10 mM HEPES, 1 mM MgCl<sub>2</sub> at pH 7.2 for magnesium experiment). Liver PI lipid mixtures were resuspended in 800  $\mu$ L of warmed buffer solution (buffer composition same as listed above). MLV mixtures were heated for 7 minutes at 65°C and vortexed for 60 seconds. 800  $\mu$ L of buffer was measured into a 2 mL vial. Lipid sample and reference buffer were degassed for 30 minutes at 10.0°C. The final total lipid concentrations were 0.15 mM for DPPI and 1 mM for Liver PI, respectively.

### 2.3 Differential Scanning Calorimetry

DSC measurements of MLVs were carried out using a Microcal VP-DSC (Northampton, MA).



**Figure 6.** Differential Scanning Calorimeter as seen in the Gericke Lab. Original photo.

Sample and reference channels were filled to ensure air bubbles were avoided. The PSI of the chambers exceeded 30. The scan rate was 60°C/hour, and the total lipid concentration was 0.15 mM for DPPI and 1 mM for Liver PI, respectively. A total of 9 scans (2-80°C) were recorded. Upscans #3, 5, 7, and 9 were used for analysis.

## 3.0 Results

### 3.1 DPPI Results

The DSC thermograms of DPPI Standard, 0.15 mM DPPI-Ca<sup>2+</sup>, and 0.15 mM DPPI-Mg<sup>2+</sup> MLVs are compared. For the DPPI standard in buffer solution a phase transition temperature of 43.6°C was observed, while in the presence of Ca<sup>2+</sup> and Mg<sup>2+</sup> the phase transition temperature shifts to 55.8°C and 51.6°C, respectively.

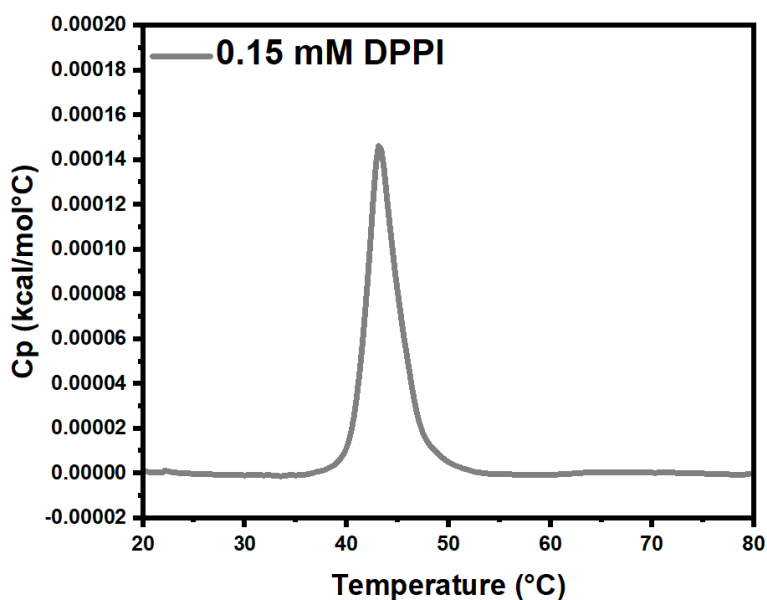


**Figure 7.** DSC thermograms of DPPI MLVs (0.15 mM total lipid concentration, average of heating scan (upscan) #3, 5, 7, and 9, heating rate = 60°C/hour, pH 7.2, 150 mM NaCl, 10 mM HEPES, 0.1 mM EDTA). The main phase transition is found at 43.6°C.

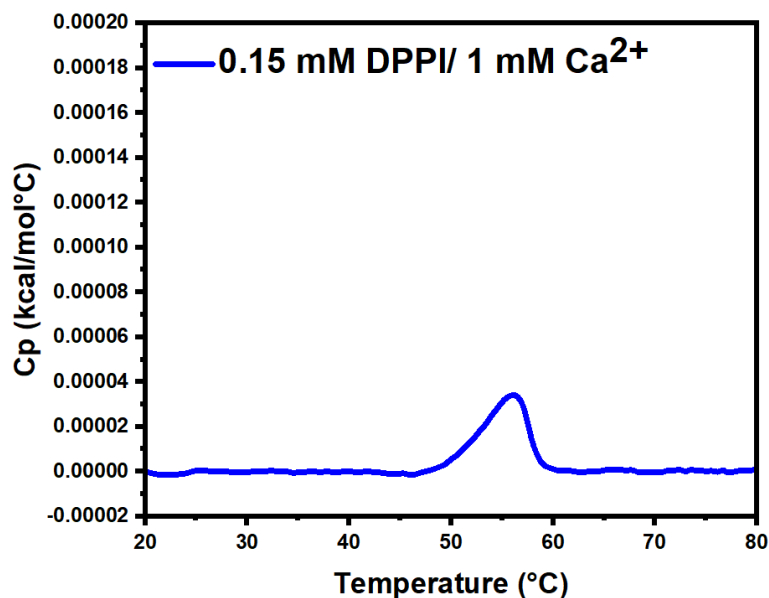


**Figure 8.** DSC thermograms of DPPI-Ca<sup>2+</sup> (blue) MLVs (0.15 mM total lipid concentration, average of heating scan (upscan) #3, 5, 7, and 9, heating rate = 60°C/hour, pH 7.2, 150 mM NaCl, 10 mM HEPES, 1 mM CaCl<sub>2</sub>). The main phase transition is found at 55.8°C.

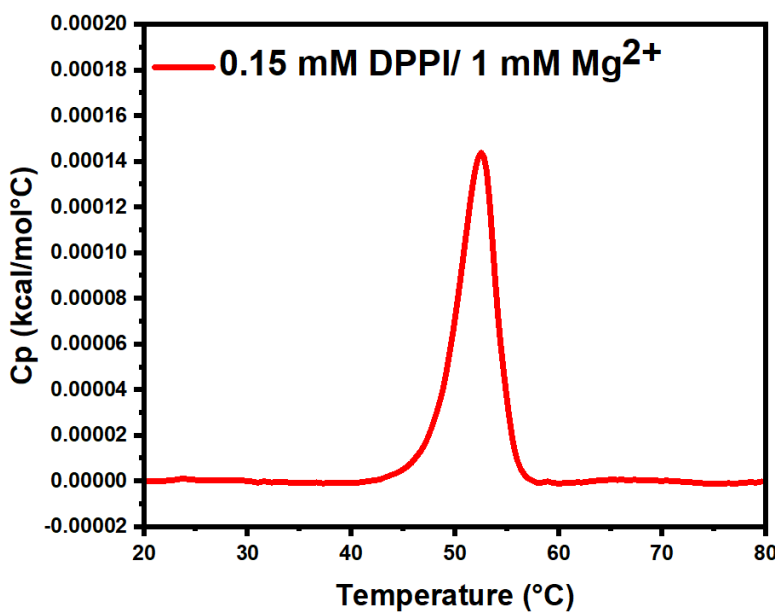


**Figure 9.** DSC thermograms of DPPI-Mg<sup>2+</sup> (red) MLVs (0.15 mM total lipid concentration, average of heating scan (upscan) #3, 5, 7, and 9, heating rate = 60°C/hour, pH 7.2, 150 mM NaCl, 10 mM HEPES, 1 mM MgCl<sub>2</sub>). The main phase transition is found at 51.6°C.

### 3.2 Liver PI Results

The DSC thermograms of 1 mM Liver PI- $\text{Ca}^{2+}$  and 1 mM Liver PI- $\text{Mg}^{2+}$  MLVs are compared. For Liver PI, we found in pH 7.2 buffer a phase transition temperature in the presence of  $\text{Ca}^{2+}$  and  $\text{Mg}^{2+}$  the phase transition temperature to be  $11.8^\circ\text{C}$  and below  $0^\circ\text{C}$ , respectively.

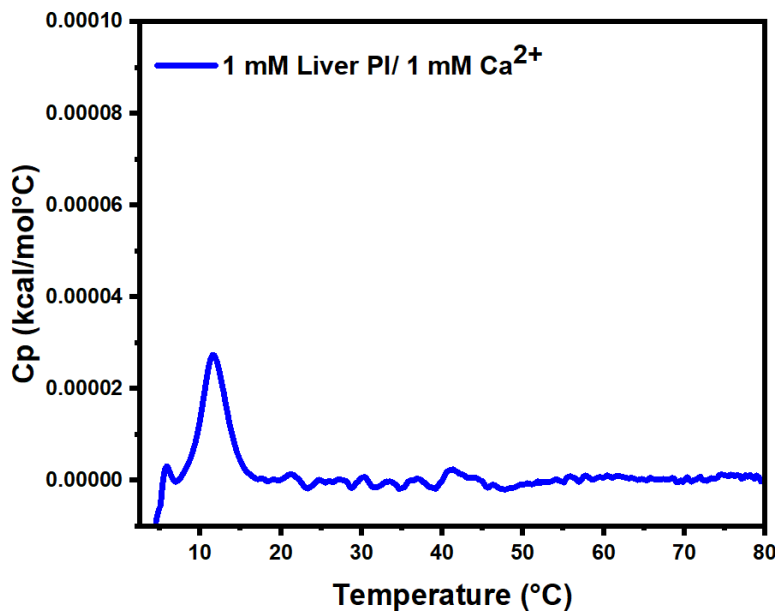


**Figure 10.** DSC thermograms of Liver PI- $\text{Ca}^{2+}$  (blue) MLVs (1 mM total lipid concentration, average of heating scan (upscan) #3, 5, 7, and 9, heating rate =  $60^\circ\text{C}/\text{hour}$ , pH 7.2, 150 mM NaCl, 10 mM HEPES, 1 mM  $\text{CaCl}_2$  for experiment). The main phase transition is found at  $11.8^\circ\text{C}$ .

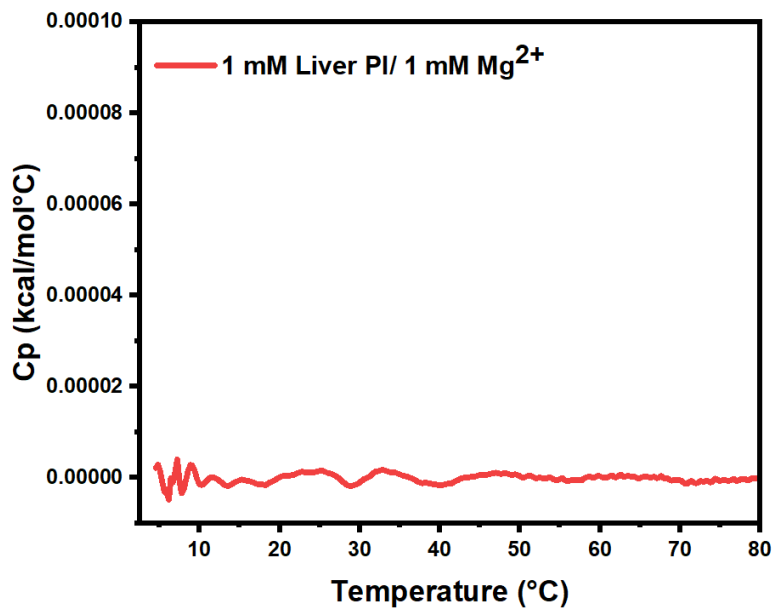


**Figure 11.** DSC thermograms of Liver PI-Mg<sup>2+</sup> (red) MLVs (1 mM total lipid concentration, average of heating scan (upscan) #3, 5, 7, and 9, heating rate = 60°C/hour, pH 7.2, 150 mM NaCl, 10 mM HEPES, 1 mM MgCl<sub>2</sub> for magnesium experiment). The main phase transition is not observed (less than 0°C).

### 3.3 Comparison of Anionic Lipids and Bivalent Cations

Consistent between both DPPI and Liver PI experiments, the addition of calcium shifts the phase transition temperature higher than the addition of magnesium.

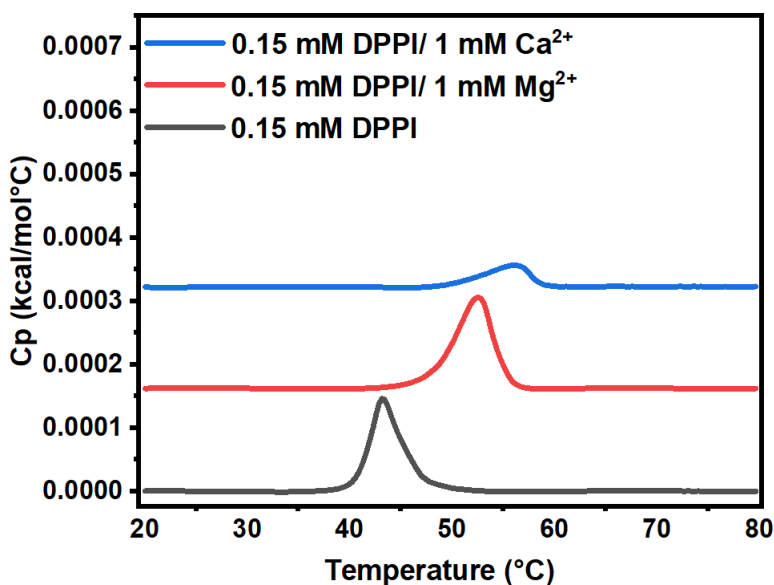


**Figure 12.** DSC thermograms of DPPI Standard (black), DPPI-Ca<sup>2+</sup> (blue), and DPPI-Mg<sup>2+</sup> (red) MLVs (0.15 mM total lipid concentration, average of heating scan (upscan) #3, 5, 7, and 9, heating rate = 60°C/hour, pH 7.2, 150 mM NaCl, 10 mM HEPES, 0.1 mM EDTA for standard experiment; 150 mM NaCl, 10 mM HEPES, 1 mM CaCl<sub>2</sub> for calcium experiment; 150 mM NaCl, 10 mM HEPES, 1 mM MgCl<sub>2</sub> for magnesium experiment).

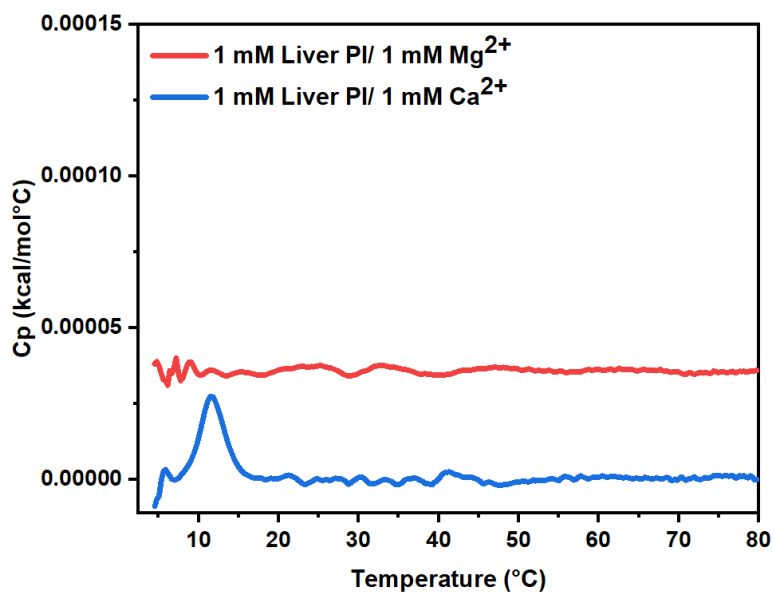


**Figure 13.** DSC thermograms of Liver PI-Ca<sup>2+</sup> (blue) and Liver PI-Mg<sup>2+</sup> (red) MLVs (1 mM total lipid concentration, average of heating scan (upscan) #3, 5, 7, and 9, heating rate = 60°C/hour, pH 7.2, 150 mM NaCl, 10 mM HEPES, 1 mM CaCl<sub>2</sub> for calcium experiment; 150 mM NaCl, 10 mM HEPES, 1 mM MgCl<sub>2</sub> for magnesium experiment).

A summation table of the gel/fluid phase transition temperature is shown below:

Sample	Gel/Fluid Phase Transition Temperature (°C)
DPPI	43.6
DPPI-Ca <sup>2+</sup>	55.8
DPPI-Mg <sup>2+</sup>	51.6
Liver PI-Ca <sup>2+</sup>	11.8
Liver PI-Mg <sup>2+</sup>	Less than 0 (not observed)

**Table 1.** Summation of the gel/fluid phase transition temperature of DPPI and Liver PI in the presence (and absence of DPPI) of Ca<sup>2+</sup> and Mg<sup>2+</sup>.

## 4.0 Discussion

### 4.1 Comparison of the Phase Transition Temperature of DPPI vs Liver PI

The phase transition temperature of Liver PI is greatly shifted downwards which can be attributed to its chemical structure. Liver PI has one saturated and one unsaturated chain whereas DPPI has two saturated chains as seen in Figure 2 and Figure 3. Unsaturated chains are unable to pack as tightly because of the rotational constraint imparted by the double bond therefore the Liver PI phase undergoes the gel/liquid-crystalline phase transition at a lower temperature. The broadening of the peak in the Liver PI thermograms indicates a less cooperative melting behavior. This is explained as Liver PI is a natural lipid mixture and has a wider array of fatty acid distribution than DPPI as shown in Figure 14.

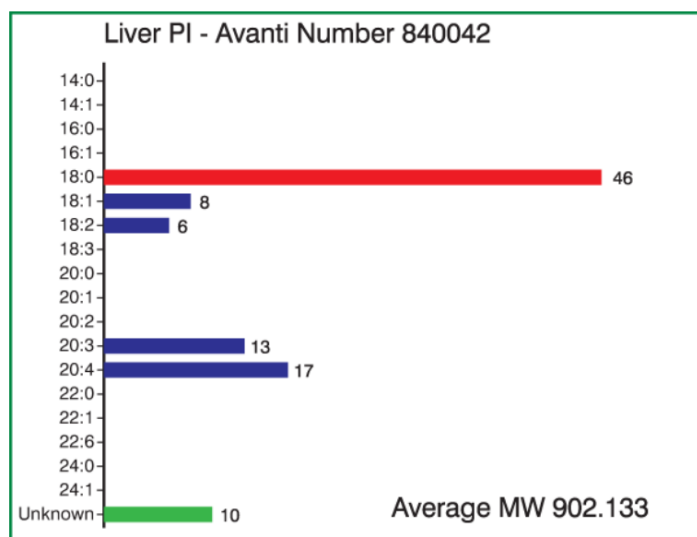


**Figure 14.** Fatty acid distribution of Liver PI from Avanti Polar Lipids [14].

The fatty acid distribution of Liver PI includes chains 18:0, 18:1, 18:2, 20:3, 20:4, and unknown where DPPI is composed of chain 16:0.

### 4.2 Comparison of the Phase Transition Temperature of Calcium vs Magnesium

Calcium binds tighter to PI than magnesium, resulting in a higher phase transition temperature. The enthalpy (integrated peak intensity) for the PI transition in the presence of  $\text{Ca}^{2+}$  is smaller than the corresponding value for  $\text{Mg}^{2+}$ . This might indicate that some kind of  $\text{PI}/\text{Ca}^{2+}$  cluster persists beyond the phase transition temperature. In addition, the melting transition in the presence of  $\text{Ca}^{2+}$  is broadened, indicating a less cooperative melting.

Understanding calcium interactions with lipids membranes at the molecular level is critical given their role in calcium signaling, protein association with cellular membranes, and membrane fusion. Calcium binding capacity is high in lipid membranes. Their bivalent properties make

them effective binders [16]. Rapid increases in calcium concentration generated by an influx are linked to key processes in calcium signaling. A number of experimental approaches have been used to investigate the interactions of calcium ions with lipid membranes. The presence of  $\text{Ca}^{2+}$  is widely considered to rigidify and organize lipid bilayers [16]. Conformation changes of the lipid headgroup, acyl chain ordering, and lipid dehydration have all been documented. Many studies show that calcium primarily binds to the phosphate group of all phospholipids regardless of charge. Simulations indicate that  $\text{Ca}^{2+}$  is able to cluster phospholipid molecules via ion-bridge [16]. Overall, it can be concluded that lipid bilayer strongly absorbs calcium ions, and calcium absorption compresses lipids bilayers as seen by the data presented in this project.

Regarding magnesium, its small size prevents direct head-to-head coordination, therefore  $\text{Mg}^{2+}$  retains the majority of its hydration shell, substituting one water molecule with a phosphate oxygen [17]. This water-mediated crosslinking is correlated to the increase in phase transition. In summary, calcium preferentially binds with the ester moiety, while magnesium binds to the phosphate group.

Studies conducted with 1,2-Dimyristoyl-sn-glycero-3-phosphocholine (DMPC) demonstrate that both bivalent cations have a strong, concentration dependent influence on transition temperatures.  $\text{Ca}^{2+}$  has the greatest effect on phase transition temperature, which is consistent with coordination of 3-4 lipids molecules [17]. In the case of  $\text{Mg}^{2+}$ , despite only directly coordinating a single lipid, it has a significant effect due to hydrogen bonds produced by water molecules in the coordination of shell to oxygen in the phosphate group of nearby lipids [17]. Although DMPC consists of a glycerol backbone linked to two fatty acids and a phosphocholine molecule, this study does give perspective regarding bivalent cation behavior which aligns with the behavior observed in this project.

## 5.0 Conclusion & Future Studies

In this project, the phase behavior of anionic lipids, DPPI and Liver PI, in the presence (in the case of DPPI, absence) of  $\text{Ca}^{2+}$  or  $\text{Mg}^{2+}$  of multilamellar vesicles was investigated. We utilized DSC to do so. This study is important as it provides a snapshot of lipids' favored behavior which in turn enhances our knowledge of how lipids may interact in the plasma membrane.

For the DPPI standard in buffer solution a phase transition temperature of  $43.6^\circ\text{C}$  was observed, while in the presence of  $\text{Ca}^{2+}$  and  $\text{Mg}^{2+}$  the phase transition temperature shifts to  $55.8^\circ\text{C}$  and  $51.6^\circ\text{C}$ , respectively. For Liver PI, we found in pH 7.2 buffer a phase transition temperature in the presence of  $\text{Ca}^{2+}$  and  $\text{Mg}^{2+}$  the phase transition temperature to be  $11.8^\circ\text{C}$  and below  $0^\circ\text{C}$ , respectively.

The phase transition temperature of Liver PI is greatly shifted downwards which can be attributed to its chemical structure. Liver PI has one saturated and one unsaturated chain whereas DPPI has two saturated chains. The broadening of the peak in the Liver PI thermograms indicates a less cooperative melting behavior. This is explained as Liver PI is a natural lipid mixture and has a wider array of fatty acid distribution than DPPI.

Calcium binds tighter to PI than magnesium, resulting in a higher phase transition temperature. The enthalpy (integrated peak intensity) for the PI transition in the presence of  $\text{Ca}^{2+}$  is smaller than the corresponding value for  $\text{Mg}^{2+}$ . This might indicate that some kind of PI/ $\text{Ca}^{2+}$  cluster persists beyond the phase transition temperature. In addition, the melting transition in the presence of  $\text{Ca}^{2+}$  is broadened, indicating a less cooperative melting.

For future studies, other PIs can be run to create a library of more PI phase transition temperatures. Additionally, we can extend this method to running and observing PIPs phase behavior as it's not as well documented. Another direction of a future study is exploring the concentration dependence of the phase transition temperature.

## 6.0 References

- [1] Nicolson, G. (2013). Update of the 1972 Singer-Nicolson Fluid-Mosaic Model of Membrane Structure. *Discoveries*. <https://doi.org/10.15190/d.2013.3>
- [2] Singer, S. J., & Nicolson, G. L. (1972). The Fluid Mosaic Model of the Structure of Cell Membranes. *Science*, 175(4023), 720–731. <https://doi.org/10.1126/science.175.4023.720>
- [3] Nicolson, G. L., & Ferreira de Mattos, G. (2021). A Brief Introduction to Some Aspects of the Fluid–Mosaic Model of Cell Membrane Structure and Its Importance in Membrane Lipid Replacement. *Membranes*, 11(12), 947. <https://doi.org/10.3390/membranes11120947>
- [4] Chan, Y.-H. M., & Boxer, S. G. (2007). Model membrane systems and their applications. *Current Opinion in Chemical Biology*, 11(6), 581–587. <https://doi.org/10.1016/j.cbpa.2007.09.020>
- [5] Feigenson, G. W. (2009). Phase diagrams and lipid domains in multicomponent lipid bilayer mixtures. *Biochimica et Biophysica Acta (BBA) - Biomembranes*, 1788(1), 47–52. <https://doi.org/10.1016/j.bbamem.2008.08.014>
- [6] Ackerman, D. G., & Feigenson, G. W. (2015). Lipid bilayers: clusters, domains and phases. *Essays in Biochemistry*, 57, 33–42. <https://doi.org/10.1042/bse0570033>
- [7] Koynova, R., & Tenchov, B. (2013). Phase Transitions and Phase Behavior of Lipids. *Encyclopedia of Biophysics*, 1841–1854. [https://doi.org/10.1007/978-3-642-16712-6\\_542](https://doi.org/10.1007/978-3-642-16712-6_542)
- [8] *Avanti Polar Lipids*. (2016). Avanti Polar Lipids. <https://avantilipids.com/product-category/phospholipids/pi-pip-lpi>
- [9] Balla, T. (2013). Phosphoinositides: Tiny Lipids With Giant Impact on Cell Regulation. *Physiological Reviews*, 93(3), 1019–1137. <https://doi.org/10.1152/physrev.00028.2012>
- [10] Gill, P., Moghadam, T. T., & Ranjbar, B. (2010). Differential scanning calorimetry techniques: applications in biology and nanoscience. *Journal of Biomolecular Techniques : JBT*, 21(4), 167–193. <https://www.ncbi.nlm.nih.gov/pmc/articles/PMC2977967/>
- [11] Cooper GM. *The Cell: A Molecular Approach*. 2nd edition. Sunderland (MA): Sinauer Associates; 2000
- [12] Garrós, N., Mallandrich, M., Beirampour, N., Mohammadi, R., Domènech, Ò., Rodríguez-Lagunas, M. J., Clares, B., & Colom, H. (2022). Baricitinib Liposomes as a New

- Approach for the Treatment of Sjögren's Syndrome. *Pharmaceutics*, 14(9), 1895.  
<https://doi.org/10.3390/pharmaceutics14091895>
- [13] *Avanti Polar Lipids*. (2018). Avanti Polar Lipids (En-US).  
<https://avantilipids.com/product/850141>
- [14] *Avanti Polar Lipids*. (2018). Avanti Polar Lipids (En-US).  
<https://avantilipids.com/product/840042>
- [15] Alberts, B., Johnson, A., Lewis, J., Raff, M., Roberts, K., & Walter, P. (2023). *The Lipid Bilayer*. Nih.gov; Garland Science.  
<https://www.ncbi.nlm.nih.gov/books/NBK26871/#:~:text=Approximate%20Lipid%20Compositions%20of%20Different,phosphatidylethanolamine%2C%20phosphatidylserine%2C%20and%20sphingomyelin.>
- [16] Adéla Melcrová, Šárka Pokorná, Saranya Pullanchery, Kohagen, M., Jurkiewicz, P., Hof, M., Jungwirth, P., Cremer, P., & Lukasz Cwiklik. (2016). The complex nature of calcium cation interactions with phospholipid bilayers. *Scientific Reports*, 6(1).  
<https://doi.org/10.1038/srep38035>
- [17] Minh, T., Aamd Hourri, Nimalka Balage, Smith, B. J., & Mechler, A. (2019). Interaction of Small Ionic Species With Phospholipid Membranes: The Role of Metal Coordination. *Frontiers in Materials*, 5. <https://doi.org/10.3389/fmats.2018.00080>
- [18] Casares, D., Escribá, P. V., & Catalina Ana Rosselló. (2019). Membrane Lipid Composition: Effect on Membrane and Organelle Structure, Function and Compartmentalization and Therapeutic Avenues. *International Journal of Molecular Sciences*, 20(9), 2167–2167. <https://doi.org/10.3390/ijms20092167>